Recovery Effects of Alginate Film and Thermal Nursing in Thoracoscopic Surgery Patients

Sen LU [1], Jie LIU [2], Juan LI [3], Shasha LI [3], Yuxia WANG [4], Xiaolong SONG [5], Xiongwei CHEN [6] *

[1] *Department of Anesthesiology, Suzhou BenQ Medical Center, The Affiliated BenQ Hospital of Nanjing Medical University, Suzhou 215010, Jiangsu Province, China*
[2] *Department of Anesthesiology, The Second Hospital of Lanzhou University, Lanzhou 730000, Gansu Province, China*
[3] *Operating Room, Shandong Provincial Hospital Affiliated to Shandong First Medical University, Jinan, Shandong, 250021, China*
[4] *Department of Stomatology, Shandong Provincial Hospital Affiliated to Shandong First Medical University, Jinan, Shandong, 250021, China*
[5] *Outpatient Service, Shandong Provincial Hospital Affiliated to Shandong First Medical University, Jinan, Shandong, 250021, China*
[6] *Wenzhou TCM Hospital of Zhejiang Chinese Medical University, Wenzhou 325000, Zhejiang Province, China*

http://doi.org/10.5755/j02.ms.41091

Received 7 April 2025; accepted 30 June 2026

The healing process of postoperative wounds is a dynamic and complex. Thoracoscopic surgery, as a new minimally invasive technique in thoracic surgery, is of great significance in exploring the postoperative recovery quality of patients undergoing this surgery. Therefore, this study uses micro controlled flow spinning technology to prepare a calcium alginate fiber coating (CaAFC) film using materials such as sodium alginate (SA). Combined with thermal insulation nursing during the recovery period, the effect of this film was explored in patients undergoing thoracoscopic general anesthesia surgery (TGAS), and it was applied in animal experiments simulating TGAS. The results showed that the permeability of the CaAFC was 93 g/m^2·24 h, the porosity was 73 %, and the water absorption rate was 21.5 g/g, demonstrating good breathability and water absorption. The relative growth rate (RGR) of HaCaT cells under CaAFC was 1.52, and the stress fiber staining intensity (SFSI) was 1.31, both of which were higher than the other two dressings. These findings indicated that the material was non-toxic to cells and could significantly improve cell activity. The wound healing rate of mice treated with CaAFC on the 15th day after surgery was 96.3 %, which was significantly higher than that of mice treated with traditional alginate medical dressings (TAMD) and medical gauze (MG). These results indicated that CaAFC could promote wound healing. The above results indicate that the CaAFC has good breathability, water absorption, and antibacterial properties. Moreover, it can significantly promote wound healing, increase cell activity, reduce postoperative infection risk, and provide support for improving postoperative care for patients undergoing thoracoscopy surgery in clinical practice.

Keywords: alginate based film application, thoracoscopic surgery, postoperative recovery, calcium alginate fiber coating, new medical dressings.

1. INTRODUCTION

In recent years, with the rapid development of medical technology, the preparation of new wound dressings has received increasing attention [1]. Traditional wound dressings have many disadvantages and cannot meet the increasing clinical demands. Traditional dressings often have poor air permeability, making it difficult to ensure gas exchange at the wound site. This can easily lead to the wound being damp and hot, affecting wound healing [2]. The water absorption of traditional dressings is also relatively limited. Their absorption capacity for wound exudate is insufficient, and dressings need to be changed frequently, increasing the risk of infection for patients [3]. Meanwhile, traditional dressings have insufficient antibacterial effects and are difficult to effectively inhibit the growth and reproduction of bacteria, which can easily lead to complications such as wound infections [4]. In response to these issues, the preparation of wound dressings using bio-based materials has gradually become a focus. Among them, alginate is a natural polysaccharide carbohydrate extracted from seaweed. Due to its good biocompatibility, biodegradability, and excellent physical and chemical properties, alginate has become an ideal medical dressing nowadays [5]. The medical membrane prepared by alginate can form a soft gel when contacted with wound exudate, providing an ideal moist environment for wound healing, promoting wound healing, and relieving wound pain [6, 7].

At present, a series of advances have been made in the research of alginate in wound healing, antibacterial properties, and biocompatibility. Luu et al. synthesized a hybrid wound dressing using alginate and nanoparticles extracted from butanol fractions, which contains a large amount of copper nanoparticles. Blood compatibility and biocompatibility tests showed that the dressing had high

* Corresponding author: X. Chen
E-mail: *ChenXiongwei@WTCMH.org.cn*

safety and good antibacterial effect [8]. Bhoopathy et al. demonstrated good blood compatibility and biocompatibility through in-vitro experiments using sodium alginate (SA), aloe vera, and sericin. In-vitro coagulation tests confirmed its hemostatic and blood absorption properties, and scratch tests demonstrated its good wound healing effect [9]. Norouzi et al. have prepared an antioxidant core/shell alginate/polycaprolactone nanofiber membrane, which is electrospun by using lotion to generate nanofiber mesh. By loading the hydrophilic antibiotic gentamicin in the hydrophilic alginate core, and surrounded by the hydrophobic polycaprolactone shell, core/shell nanofibers were generated. The results showed that the membrane had good biocompatibility, antioxidant performance, and antibacterial performance [10].

Thoracoscopic surgery is a minimally invasive surgical method. Although it has advantages such as less trauma and faster recovery compared to open surgery, it still faces some challenges in postoperative recovery [11, 12]. In view of this, this study first prepares a new type of calcium alginate fiber coating (CaAFC). The experimental design and analysis are conducted on its morphological characterization, physicochemical properties, hemostatic properties, and its impact on the activity of immortalized human epidermal cells. Then, animal experiments are conducted to simulate thoracoscopic general anesthesia surgery (TGAS), and CaAFC is combined with thermal insulation care to observe the wound healing of the animals.

The study explores the effect of the new CaAFC combined with thermal insulation nursing on wound healing in animal models after thoracoscopy surgery. The purpose of this exploration is to reduce postoperative complications and improve patient's quality of life. The innovation of the research lies in the design of a new type of dressing using microfluidic spinning technology (MFST). Compared with traditional dressings, this dressing not only has good breathability, water absorption, and antibacterial properties, but also significantly promotes wound healing, improves cell activity, and reduces the risk of postoperative infection. The combination of CaAFC application and awakening period insulation nursing significantly improves the wound healing rate and reduces postoperative complications compared to traditional nursing methods, thereby improving the quality of life of patients.

2. MATERIALS AND METHODS

2.1. Materials

Table 1 provides a specific introduction to the materials used in the experiment.

2.2. Experimental instruments

Table 2 shows the specific instrument parameters used.

2.3. Preparation of CaAFC

CaAFC was prepared using MFST, as illustrated in Fig. 1. MFST is a technique that combines the laminar flow effect of microfluidic technology with traditional wet spinning rapid prototyping to prepare micrometer sized fibers. It has many advantages that traditional spinning technology does not possess, such as no high voltage current, energy saving, safety, and simple operation. It is a fiber preparation technology. The width of the microfluidic chip channel is set to 150 – 300 μm. The depth is 40 μm. The width of the first nozzle is 100 μm. The width of the second nozzle is 150 μm. The fluid flow rate in the inner-channel is 6 μL/h. The fluid flow rate in the outer channel is 30 μL/h. The viscosity of the spinning solution is 10 – 1000 mPa·s. The concentration of the spinning solution is 1 – 10 wt.%.

Table 1. The instruments used in the experiment and their corresponding models

Material/Reagent	Nicknames or drug molecules	Purity/Grade	Manufacturer
Sodium alginate	SA	Analytical purity, 99 %	Aladdin Reagent Co., Ltd
Calcium chloride	$CaCl_2$	Analytical purity, 99 %	Sigma Aldrich, USA
Microfluidics chip	–	PDMS	Dalian institute of chemical physics
1-[4-(2-hydroxyethoxy) -phenyl]-2-hydroxy-2 methylacetone	I-2959	99 %, UV grade	Sigma Aldrich, USA
XFJ63 Silver Nanoparticles	–	Nanometre	Jiangsu Xianfeng Nanomaterial Technology Co., Ltd
Fluorescent latex microspheres	–	Diameter of 1 μm, fluorescence intensity ≥ 90 %	Sigma Aldrich, USA
Phosphate buffer saline	PBS	Aseptic (1×, pH 7.4 ± 0.1)	Sigma Aldrich, USA
Deionized water	–	Ultra-pure water (resistivity ≥ 18.2 M Ω ·cm)	Aladdin Reagent Co., Ltd

Table 2. Experimental instruments and their corresponding models

Instrument name	Model number	Manufacturer
Microfluidic pressure pump	Mitos P-Pump	Dolomite UK
Fluorescent Inverted microscope	OLYMPUS-IX73	Olympus Corporation
Scanning electron microscope (SEM)	JSM-7800F	JEOL
Vacuum filtration pump	SHZ-D II	Zhengzhou Kehua Instrument Equipment Co., Ltd
Vacuum freeze dryer	Lab-1A-80	Shanghai Precision Instrument Co., Ltd
Ultraviolet Lamp	LUYOR-2120C	Shenzhen Times Peak Technology Co., Ltd
Electronic balance	FA2204B	Shanghai Youke Instrument and Meter Co., Ltd

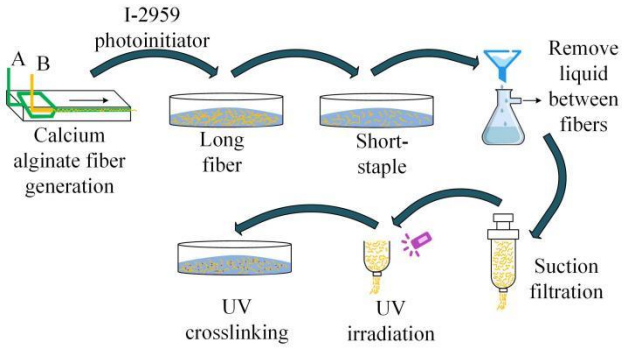

Fig. 1. Preparation of calcium alginate coating

In Fig. 1, 2 wt.% SA solution, 2 wt.% $CaCl_2$ solution, 0.5 wt.% I-2959 photoinitiator, and 2 wt% PEFDA are first prepared using distilled water solvent. A mixed spinning solution (MSS) of PEFDA and the equipped SA solution are prepared in a ratio of 1: 1, 1: 2, 2: 1, and 3: 1, and the MSS and $CaCl_2$ solution are loaded separately into a MFPP. Then, the microfluidic chip in a culture dish is fixed with a diameter of 15 cm and 80 mL of 2 wt.% $CaCl_2$ solution is injected into it. Then, the microfluidic chip is connected with two solutions in the microfluidic pressure pump through a catheter, and CaCl2 solution is injected into the microfluidic chip at a constant speed of 30 μ l/h and 6 μ l/h of mixed spinning solution respectively. Ion exchange is rapidly generated at the channel of the chip to generate gel like calcium alginate composite fiber. Finally, 20 mL of 0.5 wt.% photoinitiator is placed into a culture dish and soaked for 15 min. The fibers are cut through blade, and a vacuum filtration pump is used to filter out excess liquid. CaAFC is prepared by freeze-drying it using a vacuum freeze-drying machine.

2.4. Characterization of micro-structure of CaAFC

The microstructure of freeze-dried CaAFC was observed using field emission SEM (JSM-7800F, JEOL) at an accelerating voltage of 5 kV. Samples were fixed on the electron microscope stage and sputter-coated with gold for 30 seconds using a sputter coater. The morphological characteristics of CaAFC were also observed under a fluorescence microscope (OLYMPUS-IX73, Olympus Corporation) after staining.

2.5. Physical and chemical performance analysis

2.5.1. Water absorption performance (WAP)

To test the water absorption of CaAFC, the freeze-dried film was first weighed using an electronic balance and its weight was recorded as G_0. Then a culture dish was prepared with a diameter of 5 cm and 20 mL of distilled water was injected into it. At room temperature, the freeze-dried film was placed in a culture dish to absorb the liquid for 1 h. Finally, the film was removed, the liquid on the surface of the sample was removed through filter paper and weighed. The weight was recorded as G_1 and the water absorption rate of the film was calculated. The calculation method is shown in Eq. 1.

$$Q = \frac{G_1 - G_0}{G_0} \times 100\%, \quad (1)$$

Q is the water absorption rate [13].

2.5.2. Porosity

The porosity of CaAFC was determined using a liquid displacement method. Take a 2 cm × 2 cm film sample and weigh it. The sample is placed completely in ethanol for 30 minutes and weighed again. The porosity of the film can be calculated, as shown in Eq. 2.

$$P = \frac{M_2 - M_1}{\rho v_0} \times 100\%, \quad (2)$$

where P is the porosity; M_1 is the weight of the film placed before alcohol; M_2 is the weight of the film after being placed in alcohol; ρ is the density of ethanol; v_0 is the volume of the dressing.

2.5.3. Permeability

The water vapor permeability of CaAFC was measured at 37 ± 0.5 ℃ and 90.0 ± 2.0 % relative humidity. A 2.5 cm × 2.5 cm film sample was fixed over the opening of a glass bottle containing 5 mL of deionized water. The mass difference of the bottle before and after the experiment was measured over a period of t hours. The water vapor transmittance was calculated using Eq. 3.

$$WVT = \frac{24\Delta m}{S \cdot t}, \quad (3)$$

where WVT is the water vapor transmittance of CaAFC, measured in g/m^2·h; Δm is the difference in mass of the applied film before and after the experiment, in g; S is the area of the glass bottle mouth, in m^2; t is the experimental time, in h.

2.6. CaAFC hemostatic performance test

2.6.1. Antibacterial rate

The antibacterial activity of CaAFC with different ratios was detected by AATCC100 colony counting method. A circular film sample with a diameter of 5 mm was taken and disinfected with ultraviolet radiation for 0.5 h. Then, *Staphylococcus aureus (S. aureus)* and *Escherichia coli (E. coli)* were used as the experimental strain and the control strain. The *E. coli* and *S. aureus* used in the experiment were purchased from the China Industrial Microbial Culture Collection and Management Center, with strain numbers CICC 21529 and CICC 24114, respectively. At 37 ℃, it was placed in a test tube and stirred to prepare a 10^5 CFU/mL inoculated strain. The coated sample was incubated in the inoculated strain for 1 day at the same temperature. Next, 10 mL of disinfected deionized water was injected into the test tube and the tube was shaken for 5 minutes to separate the bacteria from the sample. Finally, the separation solution was diluted with 1 wt.% peptone. 100 μL of the diluted separation solution was evenly applied onto a nutrient agar plate culture dish and incubating at 37 ℃ for 1 day. Nutrient agar plates were prepared with the following composition: 1.0 % peptone, 0.5 % beef extract, 0.5 % sodium chloride, and 1.5 % agar, dissolved in distilled water to a final volume. The pH was adjusted to 7.2 – 7.4, with 121 ℃ autoclaving 20 min for reserve use. The inoculated strains were diluted with 1 wt.% peptone at the same temperature,

and 100 μL of the diluted solution was taken and applied to a nutrient agar plate for incubation for 1 day. The number of bacteria was recorded on two culture dishes separately, and the antibacterial rate was calculated by comparing the number of bacteria, as shown in Eq. 4.

$$I = \frac{n_c - n_s}{n_c} \times 100\%, \quad (4)$$

where I is the antibacterial rate; n_c is the number of bacteria in the diluted solution without samples; n_s is the number of bacteria in the diluted solution of the separation solution.

2.6.2. In-vitro coagulation index (IVCI)

The next step is to use the IVCI method to verify the in vitro coagulation effect of CaAFC. Firstly, traditional medical gauze (MG) will be used as the control sample, and CaAFC will be used as the experimental sample. The two samples were cut into squares with a side length of 1.0 cm. The two samples were placed in the same beaker and soaked in water at 37 ℃ for 5 minutes. Then, 5 mL of sodium citrate anticoagulant was mixed with 150 μL of $CaCl_2$ solution (0.1 mol). 100 μL of mixed blood was added to beakers for incubation. After 5 minutes, 20 mL of deionized water was injected into the beaker and the absorbance of the superliquid was measured by spectrophotometry at 0.545 μm using Shimazu UV-1900i double beam UV-visible spectrophotometer. Then, 20 mL of deionized water was injected into 100 mL of mixed blood, the absorbance was calculated, and this absorbance was used as a reference to calculate the in IVCI of the sample, as shown in Eq. 5.

$$BCI = \frac{A_s}{A_b} \times 100\%, \quad (5)$$

where BCI is the in IVCI value of the sample; A_s is the absorbance calculated when there is a sample present; A_b is the absorbance calculated when there is no sample.

2.6.3. Antioxidant properties

The antioxidant activity of CaAFC was measured using a free matrix external antioxidant experiment using 1,1-Diphenyl-2-picrylhydrazyl (DPPH). Firstly, DPPH radicals were mixed with ethanol solution to prepare 4 ml of 100 μM DPPH ethanol solution. At a temperature of 20 ℃, 20 mg of CaAFC was taken and placed in for 1 hour of reaction. Using the DPPH solution without sample placement as a reference, the absorbance of the two solutions was measured by spectrophotometry at 517 nm. The antioxidant properties of the film were calculated by absorbance, and the specific expression is Eq. 6.

$$RSA = \frac{A_c - A_e}{A_c} \times 100\%, \quad (6)$$

where RSA is the DPPH radical scavenging activity; A_c is the absorbance of DPPH solution without sample placement; A_e is the absorbance of the DPPH ethanol solution inserted into the sample.

2.7. Effect of CaAFC on cell growth activity

To test whether the equipped CaAFC is toxic to humans, the CCK-8 method was used to detect the activity of HaCaT under different conditions. HaCaT cells are derived from the peripheral normal skin of a 62 year old male with melanoma and are naturally transformed into immortalized human keratinocytes after in-vitro culture. The reagent kit used in the CCK method was purchased from Tongren Chemical Research Institute in Japan, with item number C0038. Firstly, the HaCaT cells would be revived and the revived cells would be seeded onto a 96 well plate. 3,000 cells were inoculated into each well and incubated for 0.5 days at a temperature of 37 ℃ and a CO_2 concentration of 5 %. Next, 2 g of CaAFC sample was taken and disinfected by irradiating it with ultraviolet light for 4 hours. It was soaked in 20 mL of Dulbecco's modified eagle medium (DMEM) containing various amino acids and glucose for 2 days 10 % fetal bovine serum was added to DMEM and cultured in a 37 ℃, 5 % CO_2 incubator. The next step was to extract the sample in DMEM medium and add it to the incubated HaCaT cells for 3 days. Finally, F-actin actin was used for staining and absorbance was calculated. The absorbance of DMEM culture medium was calculated without adding samples as a reference. The relative growth rate (RGR) of cells could be calculated based on absorbance to determine the effect of membrane application on cell growth activity. The absorbance at a wavelength of 450 nm was measured using a Multiskan GO enzyme-linked immunosorbent assay reader purchased from Thermo Fisher Scientific, and the relative cell growth rate was calculated. The experiment was repeated three times to eliminate accidental errors. The calculation method for RGR is shown in Eq. 7.

$$R = \frac{A_t}{A_f}, \quad (7)$$

Where R is the RGR; A_t is the absorbance of the applied film; A_f is the absorbance of DMEM culture medium without sample addition [14].

3. RESULTS AND DISCUSSION

3.1. Morphological changes of membrane fibers under different preparation ratios

To explore the various properties of CaAFC, the experiment first analyzed its microstructure. Fig. 2 shows SEM images of each stage of CaAFC. Fig. 2 a shows long fibers coated with calcium alginate. Among them, calcium alginate fibers (CAFs) are continuous and have uniform thickness. Fig. 2 b shows the CAFs after exposure to ultraviolet light. The fibers are interlaced and overlapped with each other, and their arrangement presents a disordered state. Fig. 2 c and d show the coated fibers after vacuum filtration. CaAFC exhibits specific directionality, which is due to the influence of shear force on the fibers during filtration, resulting in the arrangement of the filtered fibers along the membrane.

Fig. 3 shows the morphological characteristics of CaAFC under a fluorescence microscope. Fig. 3 a shows the CAFs image. In a water absorbing state, the fibers are smooth and full, and the outer surface is relatively smooth. Fig. 3 b shows the short fibers cut with a blade. The fibers overlap with each other and are arranged in disorder. Fig. 3 c and d are fibers stained with fluorescence.

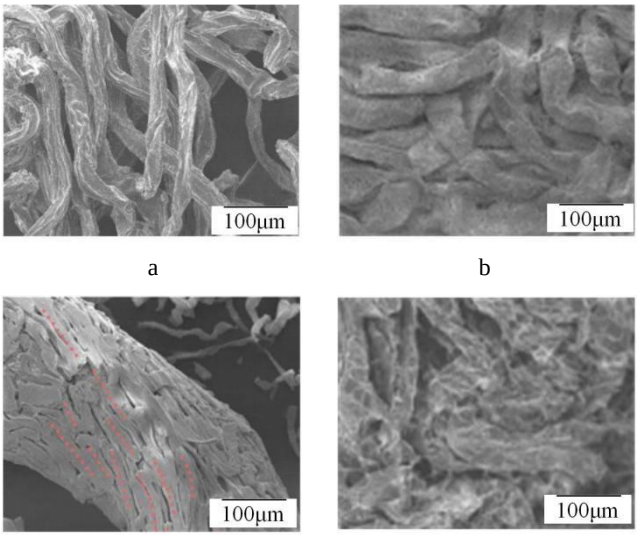

Fig. 2. SEM images of CaAFC: a – long fibers coated with calcium alginate; b – CAFs after exposure to ultraviolet light; c, d – the coated fibers after vacuum filtration

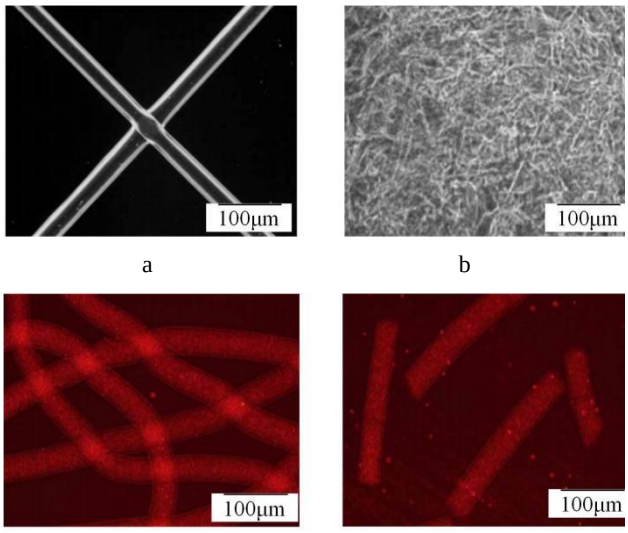

Fig. 3. Morphological characteristics of CaAFC under fluorescence microscopy: a – CAFs; b – the short fibers cut with a blade; c, d – fibers stained with fluorescence

The results presented under the fluorescence microscope were similar to those of SEM images, demonstrating the effectiveness of the designed CaAFC preparation method.

3.2. Analysis of physical and chemical properties of CaAFC

The experiment determines the physical and chemical properties of the designed film by measuring its WAP. Fig. 4 shows the results of MSSs with different ratios after absorbing distilled water for 1 hour at room temperature. In Fig. 4, when the ratio of the MSS is 1:2, its WAP is 21.5 g/g after absorbing distilled water for 1 hour. When the configuration ratio is 1:1, 2:1, and 3:1, after absorbing distilled water for 1 hour, the WAP of the prepared film is 17.1 g/g, 13.6 g/g, and 6.7 g/g.

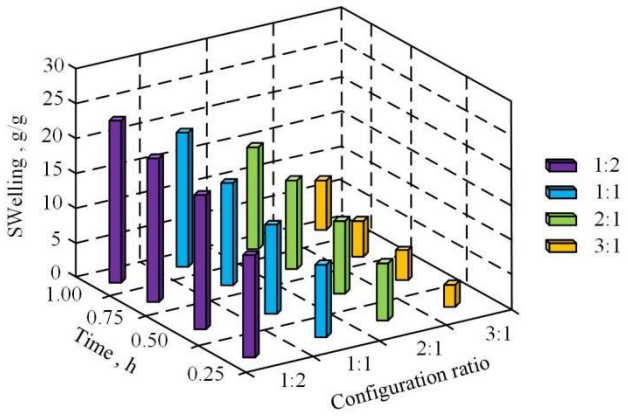

Fig. 4. Water absorption performance (WAP) of CaAFC with different MSS ratios

Therefore, with the increase of SA solution content, WAP shows an upward trend. When the MSS ratio is 1:2, the maximum WAP is 21.5 g/g. The above results indicate that the higher the PEGDA content in MSS, the smaller the WAP. This means that PEGDA can strengthen the connection between the coated fibers, reduce the pores between the fibers, and thereby reducing the water storage capacity.

The experiment further verifies the physical and chemical properties of the designed film by comparing the porosity and breathability of CaAFC, traditional alginate medical dressings (TAMD), and MG. Fig. 5 shows the comparison results.

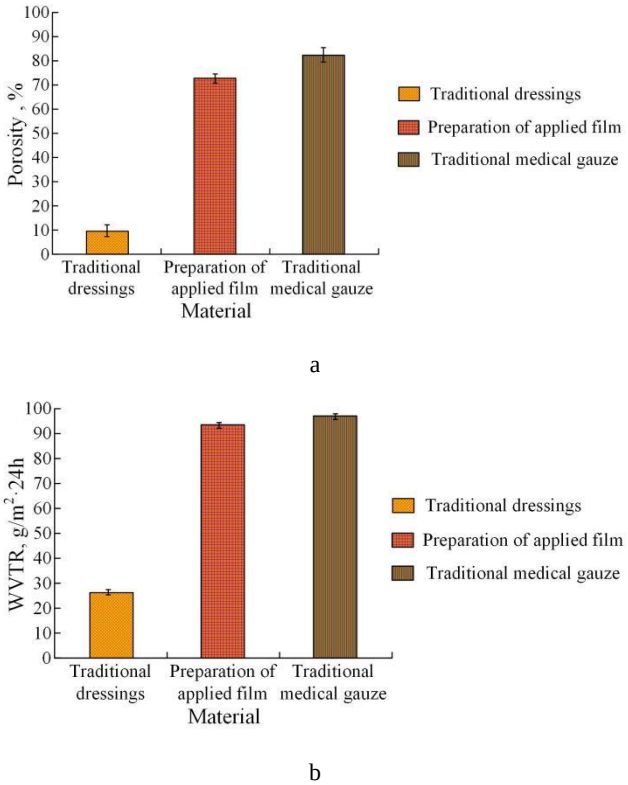

Fig. 5. Comparison of porosity and breathability of CaAFC, TAMD, and MG: a – porosity; b – breathability

In Fig. 5 a, the porosity of CaAFC, TAMD, and traditional MG is around 73 %, 10 %, and 82 %. The porosity of CaAFC is between TAMD and traditional MG,

which proves its ability to absorb wound exudate well and further proves its good water absorption ability. In Fig. 5 b, the permeability of CaAFC, TAMD, and traditional MG is approximately 93 g/m^2·24 h, 28 g/m^2·24 h, and 97 g/m^2·24 h, respectively. The breathability of CaAFC is still between the other two dressings, indicating that it can promote oxygen exchange at the wound site and promote wound healing.

3.3. Analysis of hemostatic performance of CaAFC

As demonstrated in Fig. 6, the experiment utilizes *E. coli* as a control and calculates the antibacterial rate of CaAFC against *E. coli* according to the established antibacterial testing method.

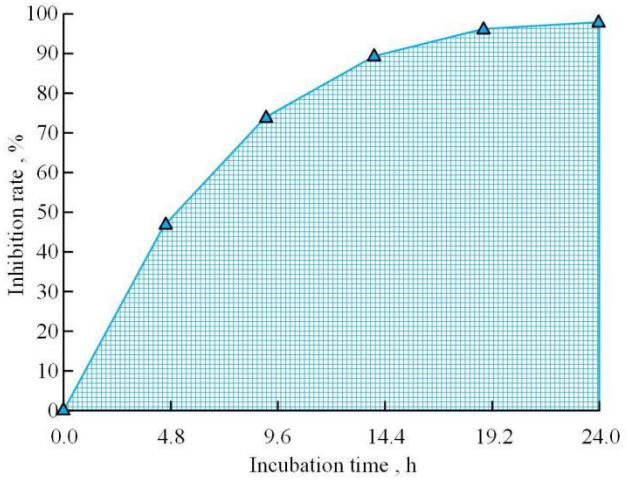

a

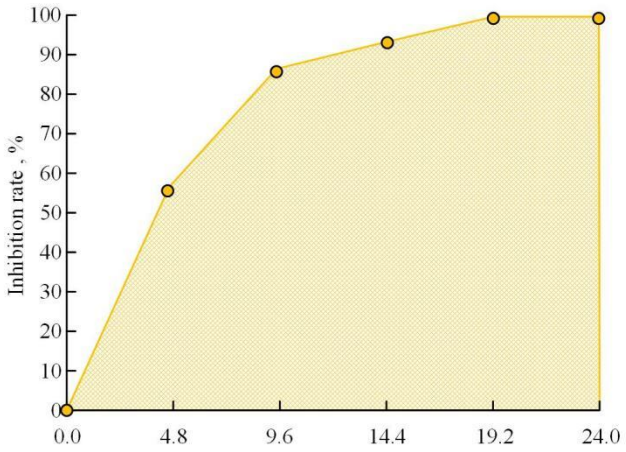

b

Fig. 6. Antibacterial rate of CaAFC against different bacteria

This calculation is then compared with the antibacterial rate of *S. aureus*. As the cultivation time increases, the antibacterial rate of CaAFC against *E. coli* and *S. aureus* gradually increases. In Fig. 6 a, after cultivation is completed, the designed film has an antibacterial rate of about 97 % against *E. coli*. In Fig. 6 b, after cultivation, the antibacterial rate of CaAFC against *S. aureus* is around 99 %. The above results demonstrate that CaAFC has good antibacterial ability.

When verifying the coagulation effect of the designed film through in IVCI, the higher the absorbance value, the worse the coagulation effect. Fig. 7 shows the variation of in-vitro coagulation indices of CaAFC, TAMD, and MG over time. In Fig. 7, the IVCI of traditional MG, TAMD, and CaAFC are 90.72 %, 51.82 %, and 35.56 %. The IVCI of the designed film is significantly smaller than the other two dressings, indicating that it can promote blood coagulation and help stop bleeding.

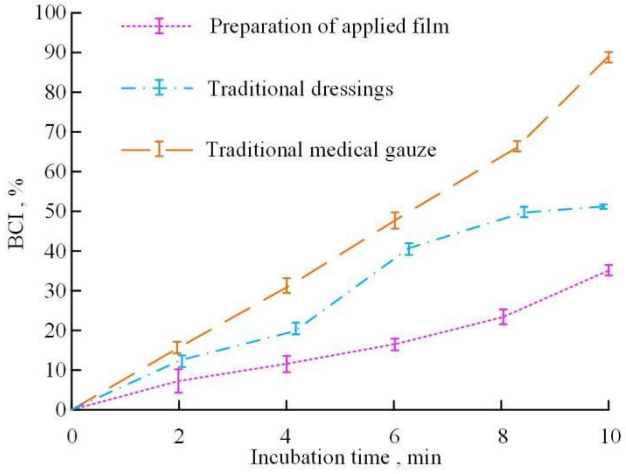

Fig. 7. IVCI of different dressings

Fig. 8 shows the changes in antioxidant indices of CaAFC, TAMD, and MG over time. In Fig. 8, as the reaction progresses, the antioxidant properties of different excipients all increase.

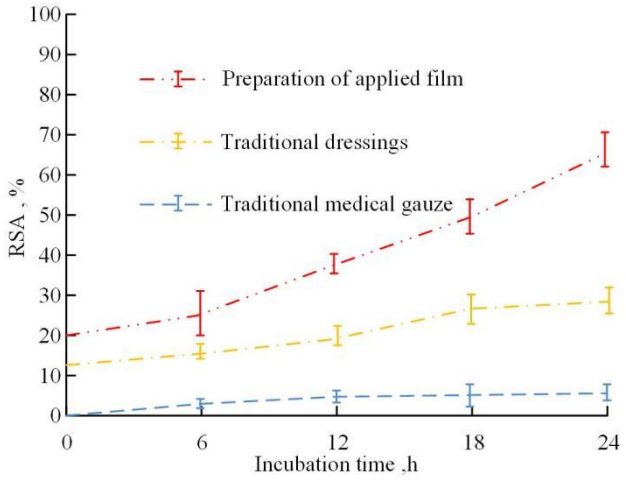

Fig. 8. Antioxidant activity of different dressings

After the reaction, the antioxidant activity of MG is about 7 %, TAMD is about 29 %, and CaAFC is about 66 %. The antioxidant performance of CaAFC is significantly higher than the other two dressings, indicating that it can reduce cell damage and improve the speed of wound recovery.

3.4. Analysis of the effect of CaAFC on cell activity

The experiment detects the effect of CaAFC on cell activity by calculating the RGR and stress fiber staining intensity (SFSI) of HaCaT cells, and compares them with

the two indicators of TAMD and MG. Fig. 9 shows the comparison results.

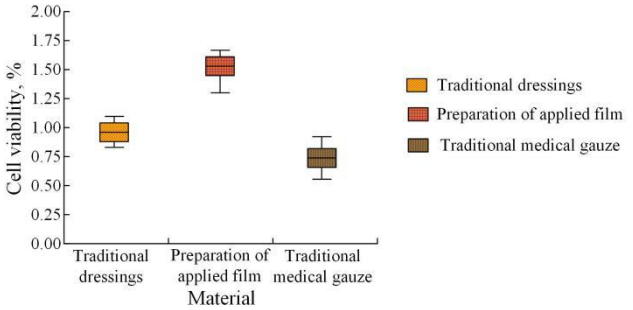

a

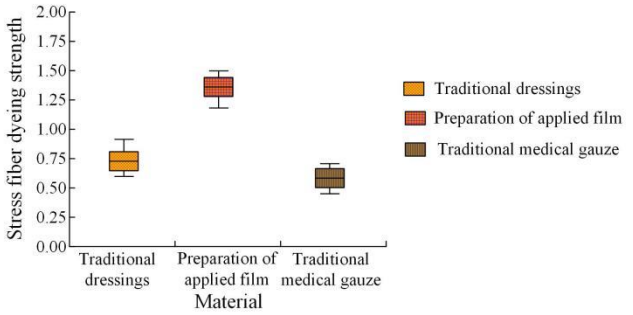

b

Fig. 9. RGR and SFSI of cells under different dressings: a – RGR; b – SFSI

In Fig. 9 a, the RGRs of HaCaT cells under CaAFC, TAMD, and MG are 1.52, 0.96, and 0.75, respectively. In Fig. 9 b, the SFSI of HaCaT cells under three different dressings is 1.31, 0.74, and 0.57, respectively. The RGR and SFSI of HaCaT cells under CaAFC are higher than those of other dressings, indicating that it can enhance cell activity and prove its non-toxic effect on the human body.

3.5. Analysis of the recovery effect of CaAFC combined with awakening period thermal insulation nursing on TGAS patients

To verify the recovery effect of CaAFC combined with thermal insulation nursing during the recovery period on TGAS patients, this study conducted animal experiments on mice. The experimental protocol has been approved by the Animal Ethics Committee, with ethics approval number JQ20240501. 24 male C57BL/6J mice aged 6 – 8 weeks and weighing 18 – 22 g were selected and anesthetized by intraperitoneal injection of 10 % chloral hydrate solution before the experiment. The skin was shaved and prepared in the center of the mouse's back, disinfected with 75 % alcohol. A sterile circular biopsy puncture device was used to remove the entire layer of skin in the center of the shaved and disinfected back, forming a circular wound with a diameter of 6 mm. The depth of the wound reached the dermis layer, but did not harm the muscles. The entire wound was covered with CaAFC, TAMD, and MG separately, replacing every 2 days. Before using dressings, the wound was carefully cleaned. At the same time, a blank control group was set up, which was the control group without using any dressings. The mice were placed in a constant temperature and ventilated insulated box. The entire experiment followed the principle of sterile operation. The size of mouse wounds under different dressings was measured on the 5th, 10th, and 15th day of the experiment, and compared with the initial size. Fig. 10 shows the degree of wound healing in mice.

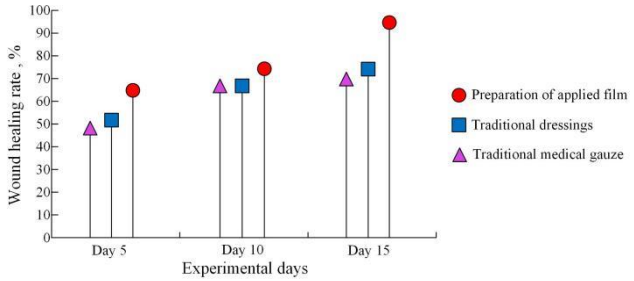

Fig. 10. Healing degree of mouse wounds under different dressings

According to Fig. 10, at the 15th day of the experiment, the wound healing rate of mice treated with CaAFC was 96.3 %, the blank control group was 58.1 %, the MG group was 69.4 %, and the TAMD group was 74.8 %. The wound healing rate of mice treated with CaAFC was significantly higher than that of mice treated with other dressings, proving that CaAFC can shorten the recovery time of patients and demonstrate its applicability in postoperative recovery under TGAS.

3.6. Discussion

This study demonstrated the potential of a novel CaAFC film, fabricated using MFST, combined with thermal management, to enhance wound healing after TGAS. The CaAFC film exhibited favorable physical and chemical properties, including high water vapor permeability, porosity, and water absorption, which are essential for creating a moist wound environment conducive to healing. High water vapor permeability ensures oxygen exchange at the wound site, while porosity and water absorption enable the dressing to effectively absorb wound exudate, preventing the wound from becoming too dry or too wet, thereby providing a favorable microenvironment for wound healing. The incorporation of PEGDA into the CaAFC film at an optimized SA:PEGDA ratio of 1:2 enhanced its water absorption capacity.

The CaAFC film also demonstrated significant antibacterial activity against E. coli and S. aureus, two common pathogens associated with wound infections. This antibacterial effect may be attributed to the presence of Ca^{2+} ions, which can disrupt bacterial cell membranes [15]. The improved in vitro coagulation observed with CaAFC is likely due to the release of Ca^{2+} ions, which play a crucial role in the coagulation cascade [16]. Furthermore, the high antioxidant activity of CaAFC may contribute to wound healing by reducing oxidative stress and promoting cell proliferation [17]. These in vitro findings are consistent with previous studies demonstrating the beneficial effects of alginate-based materials on wound healing [8 – 10, 15, 16, 18].

The in vitro cell culture experiments demonstrated that CaAFC extracts promoted HaCaT cell proliferation and stress fiber formation, indicating good biocompatibility and

the potential to stimulate cellular activity at the wound site. This is consistent with the known biocompatibility of alginate [8, 9].

The in vivo results further confirmed the efficacy of CaAFC in promoting wound healing. Mice treated with CaAFC and receiving thermal insulation exhibited significantly accelerated wound closure compared to those treated with TAMD, MG, or no dressing. Thermal management likely contributed to improved healing by promoting blood flow, reducing inflammation, and optimizing cellular activity.

This study has some limitations. The in vivo experiments were conducted on a relatively small number of animals, and only one type of wound (full-thickness excisional wound) was investigated. Further studies are needed to evaluate the efficacy of CaAFC in different wound types and larger animal models. Additionally, the long-term effects of CaAFC on wound healing and scar formation were not assessed. Only the environmental temperature control during the awakening period was studied. In the future, the influence of vital signs such as heart rate and blood pressure of patients during the awakening period on postoperative recovery will be further explored, or the role of respiratory function monitoring indicators such as respiratory rate and blood oxygen saturation of patients during the awakening period on wound healing, in order to optimize the perioperative management plan more precisely and provide support for clinical treatment.

4. CONCLUSIONS

At present, thoracoscopic surgery is a common surgical method, and the recovery effect of patients after surgery is affected by various factors. To explore the application effect of alginate-based film application combined with awakening care in TGAS patients, this study prepared a CaAFC using MFST. Its various properties were tested and compared with other commonly used medical dressings. Meanwhile, the recovery effect of the designed dressing combined with awakening care in TGAS patients was simulated through animal experiments. The results showed that the air permeability of CaAFC was 93 g/m^2·24 h, and the water absorption rate was 21.5 g/g. The result indicated that the material exhibited favorable air permeability and water absorption properties, which can facilitate the establishment of a moist wound environment, thereby promoting wound healing. The antibacterial rates of CaAFC against *E. coli* and *S. aureus* reached 97 % and 99 %, respectively, significantly higher than those of TAMDs and MG, indicating its effectiveness in reducing the risk of postoperative infection. When utilizing CaAFC, the RGR of HaCaT cells was 1.52, and the SFSI was 1.31, both of which were higher than the other two dressings. This finding indicated that CaAFC was non-toxic to cells and could significantly improve cell activity, promoting wound healing. CaAFC has good biocompatibility and can bind well with tissues without causing adverse immune reactions. In animal experiments, the wound healing rate of mice using CaAFC on the 15th day after surgery was 96.3 %, significantly higher than that of mice using TAMDs and MG, indicating that CaAFC can significantly promote wound healing and shorten the recovery time of patients. Although the research results showed a significant effect of CaAFC in the recovery of patients undergoing TGAS, its effectiveness in different types of wounds has not been experimentally tested. In future research, the experimental scope will be expanded to evaluate its application effectiveness in different wound types, aiming to ensure the universality and clinical effectiveness of CaAFC.

Ethical Compliance

This experiment involves animals, and animal experiments were conducted in accordance with the guidelines and approved by the Animal Ethics Committee of Jishou Qingyuan Biotechnology Co., Ltd. (Approval Number: JQ20240501).

REFERENCES

1. **McDill, H., Maskell, N.** Setting up a Pleural Disease Service *Clinics in Chest Medicine* 42 (4) 2021: pp. 611 – 623. https://doi.org/10.1016/j.ccm.2021.07.004
2. **Sawyer, M.P., Yong, E.X., Marginson, B., Farrell, S.G., Derbyshire, M.M., MacIsaac, R.J., Sachithanandan, N.** Utility of Semi-Quantitative Quick Cortisol Assay with Low-Dose Adrenocorticotropic Hormone Infusion Adrenal Vein Sampling *ANZ Journal of Surgery* 92 (3) 2022: pp. 437 – 442. https://doi.org/10.1111/ans.17352
3. **Santanakrishnan, R., Murali, G.S., Javaregowda, D., Shankar, G., Babu, N., Jadhav, V.** Thoracoscopy in Stage 3 Empyema Thoracis in Children–a Safe and Feasible Alternative to Thoracotomy *Journal of Pediatric Surgery* 55 (4) 2020: pp. 756 – 760. https://doi.org/10.1016/j.jpedsurg.2019.08.007
4. **El-Ghoul, Y., Alminderej, F.M.** Bioactive and Superabsorbent Cellulosic Dressing Grafted Alginate and Carthamus Tinctorius Polysaccharide Extract for the Treatment of Chronic Wounds *Textile Research Journal* 91 (3 – 4) 2021: pp. 235 – 248. https://doi.org/10.1177/0040517520935213
5. **Peters, R.T., Parikh, D.H., Singh, M.** Thoracoscopic Debridement for Empyema Thoracis *Journal of Pediatric Surgery* 55 (10) 2020: pp. 2187 – 2190. https://doi.org/10.1016/j.jpedsurg.2020.02.004
6. **Xu, P., Chang, X., Tang, S., Li, S., Cao, G., Zhang, X., Chi, S., Fang, M., Yang, D., Li, X.** Robot-Assisted Thoracoscopic Plication for Diaphragmatic Eventration *Journal of Pediatric Surgery* 55 (12) 2020: pp. 2787 – 2790. https://doi.org/10.1016/j.jpedsurg.2020.06.034
7. **Best, S., Ammons, C.L., Karunanayake, G.A., Saemundsson, S.R., Tawil, P.Z.** Outcome Assessment of Teeth with Necrotic Pulps and Apical Periodontitis Treated with Long-Term Calcium Hydroxide *Journal of Endodontics* 47 (1) 2021: pp. 11 – 18. https://doi.org/10.1016/j.joen.2020.09.005
8. **Luu, N.D.H., Nguyen, M.N., Dang, L.H., Le, T.P., Doan, T.L., Nguyen, T.T.T., Le, H.K., Nguyen, M.T., Hoang, L., Tran, N.Q.** Antibacterial and Biocompatible Wound Dressing Based on Green-Synthesized Copper Nanoparticles and Alginate *Journal of Materials Research* 39 (6) 2024: pp. 955 – 967. https://doi.org/10.1557/s43578-024-01283-y
9. **Bhoopathy, J., Sathyaraj, W.V., Yesudhason, B.V., Rajendran, S., Dharmalingam, S., Seetharaman, J.,**

Muthu, R., Murugesan, R., Raghunandhakumar, S., Anandasadagopan, S.K. Haemostatic Potency of Sodium Alginate/Aloe Vera/Sericin Composite Scaffolds – Preparation, Characterisation, and Evaluation *Artificial Cells Nanomedicine and Biotechnology* 52 (1) 2024: pp. 35 – 45. https://doi.org/10.1080/21691401.2023.2293784

10. **Norouzi, M.R., Ghasemi-Mobarakeh, L., Itel, F., Schoeller, J., Fashandi, H., Fortunato, G., Rossi, R.M.** Dual Functional Antibacterial-Antioxidant Core/Shell Alginate/Poly(E-Caprolactone) Nanofiber Membrane: A Potential Wound Dressing *ACS Omega* 9 (23) 2024: pp. 25124 – 25134. https://doi.org/10.1021/acsomega.4c02510
11. **Sundaralingam, A., Bedawi, E.O., Harriss, E.K., Munavvar, M., Rahman, N.M.** The Frequency, Risk Factors, and Management of Complications from Pleural Procedures *Chest* 161 (5) 2022: pp. 1407 – 1425. https://doi.org/10.1016/j.chest.2021.11.031
12. **Takeda, F.R., Tustumi, F., Sallum, R.A., Ribeiro, U., Cecconello, I.** Transthoracic Esophagectomy by Thoracoscopy with Pleural Repair (T-Tepler Technique): A Prospective Comparative Study to Minimize Postoperative Complication *Journal of the American College of Surgeons* 231 (4) 2020: pp. S295 – S296. https://doi.org/10.1016/j.jamcollsurg.2020.07.437
13. **Hirose, K., Sasatsu, M., Toraishi, T., Onishi, H.** Novel Xyloglucan Sheet for the Treatment of Deep Wounds: Preparation, Physicochemical Characteristics, and in Vivo Healing Effects *Biological and Pharmaceutical Bulletin* 42 (8) 2019: pp. 1409 – 1414. https://doi.org/10.1248/bpb.b18-00764
14. **Seyrek, Y., Akkuş, M.** How to Facilitate Concurrent Lower Lobectomy after Coronary Artery Bypass Grafting Via Median Sternotomy without Adding Anterolateral Thoracotomy? *ANZ Journal of Surgery* 93 (6) 2023: pp. 1559 – 1563. https://doi.org/10.1111/ans.18494
15. **Mohamed, R., El-Beheri, N.G., Agwa, M.M., Eltaher, H.M., Alseqely, M., Sadik, W.S., El-Khordagui, L.** Antibiotic-Free Combinational Hyaluronic Acid Blend Nanofibers for Wound Healing Enhancement *International Journal of Biological Macromolecules* 167 2021: pp. 1552 – 1563. https://doi.org/10.1016/j.ijbiomac.2020.11.109
16. **Ma, W., Ling, S., Liu, Y., Chen, Z., Xu, J.** Bio-Inspired Low-Cost Fabrication of Stretchable, Adhesive, Transparent, and Multi-Functionalized Joint Wound Dressings *ACS Applied Materials & Interfaces* 15 (19) 2023: pp. 22915 – 22928. https://doi.org/10.1021/acsami.3c02065
17. **Zhou, M., Gong, J., Ma, J.** Continuous Fabrication of near-Infrared Light Responsive Bilayer Hydrogel Fibers Based on Microfluidic Spinning *e-Polymers* 19 (1) 2019: pp. 215 – 224. https://doi.org/10.1515/epoly-2019-0022
18. **Yin, M., Wan, S., Ren, X., Chu, C.** Development of Inherently Antibacterial, Biodegradable, and Biologically Active Chitosan/Pseudo-Protein Hybrid Hydrogels as Biofunctional Wound Dressings *ACS Applied Materials & Interfaces* 13 (12) 2021: pp. 14688 – 14699. https://doi.org/10.1021/acsami.0c21680